Journal of Power Sources 213 (2012) 180–185

Contents lists available at SciVerse ScienceDirect

Journal of Power Sources

journal homepage: www.elsevier.com/locate/jpowsour

Li-ion capacitors with carbon cathode and hard carbon/stabilized lithium metal powder anode electrodes

W.J. Cao [a], J.P. Zheng [a,b,*]

[a] Department of Electrical and Computer Engineering, Florida A&M University and Florida State University, Tallahassee, FL 32310, USA
[b] Center for Advanced Power Systems (CAPS), Florida State University, Tallahassee, FL 32310, USA

ARTICLE INFO

Article history:
Received 7 February 2012
Received in revised form
14 April 2012
Accepted 16 April 2012
Available online 21 April 2012

Keywords:
Li-ion capacitors
Stabilized lithium metal powders
Hard carbon
Activated carbon

ABSTRACT

A lithium-ion capacitor was developed using a mixture of stabilized lithium metal powder and hard carbon as the anode electrode, while activated carbon was used as the cathode. A specific energy of approximately 82 Wh kg^{-1} was obtained based on the weight of electrode materials; however, when the electrolyte, separator, and current collectors were included, the specific energy of an assembled Li-ion capacitor was about 25 Wh kg^{-1}. The capacitor was able to deliver over 60% of the maximum energy at a discharge C-rate of 44C. Through continuous galvanostatic charge/discharge cycling, the capacitance of the Li-ion capacitor degraded less than 3% over 600 cycles.

1. Introduction

The biggest challenge facing electrochemical (EC) capacitors is how to significantly increase the energy density of the cell. A significant amount of work has been done in understanding the relationship of the pore size to the ionic accessibility from the electrolyte and developing various pseudocapacitance materials in order to maximize the charge storage capability [1–4]; however, there are limited studies on charge storage mechanisms such as the active role the electrolyte plays during the charge and discharge process: ion separation or ion shutter. In double-layer capacitors, the ionic concentration in the electrolyte increases and decreased during charge and discharge, respectively. The energy density theory guide clearly shows that the energy densities for both double-layer capacitors and asymmetrical cells are mainly limited by how many ions are available in the electrolyte or the salt concentration in the electrolyte [5–8,11], because the minimum amount of required ions in the electrolyte is equal to the maximum charge capacity of the electrode in a capacitor. In contrast, for lithium (Li)-ion batteries, the Li-ions shutter between two electrodes and the concentration keeps a constant value during charge and discharge; therefore, a high energy density cell can be obtained. From previous theoretical and experimental studies, it has been concluded that the energy density for both conventional EC double-layer capacitors or asymmetrical cells must be much less than that of advanced batteries, due to the fundamental difference between these two systems, in which the EC double-layer capacitors and asymmetrical cells consume the salt in electrolyte during the charge process unlike the advanced batteries which do not. In EC double-layer capacitors and asymmetrical cells, the minimum weight of the required electrolyte in the cell is even greater than the weight of both electrode materials; however; in advanced batteries, the ion concentration in the electrolyte remains constant during the entire charge and discharge process, and there is no net ion exchange between the electrode and the electrolyte.

In this paper, we demonstrate a Li-ion capacitor which is capable of achieving high energy density, long cycle life and high power density. The Li-ion capacitor consists of a battery electrode with Li intercalated hard carbon anode and a double-layer cathode electrode with the open-circuit potential at or near the maximum potential when the cell is fully charged. Fig. 1 illustrates the charge transfer during the first charge or discharge processes for EC double-layer capacitors and the Li-ion capacitors. It can be seen that for EC double-layer capacitors, during charge, electrons move from the positive electrode to the negative electrode through the external load, at the same time, ions are separated from the bulk electrolyte and accumulated near the electrode surface; during the discharge, these electrons move from the negative electrode to the positive electrode, and ions are released from the electrode surface

* Corresponding author. Department of Electrical and Computer Engineering, Florida A&M University and Florida State University, Tallahassee, FL 32310, USA.
E-mail address: zheng@eng.fsu.edu (J.P. Zheng).

0378-7753/$ – see front matter © 2012 Elsevier B.V. All rights reserved.
doi:10.1016/j.jpowsour.2012.04.033

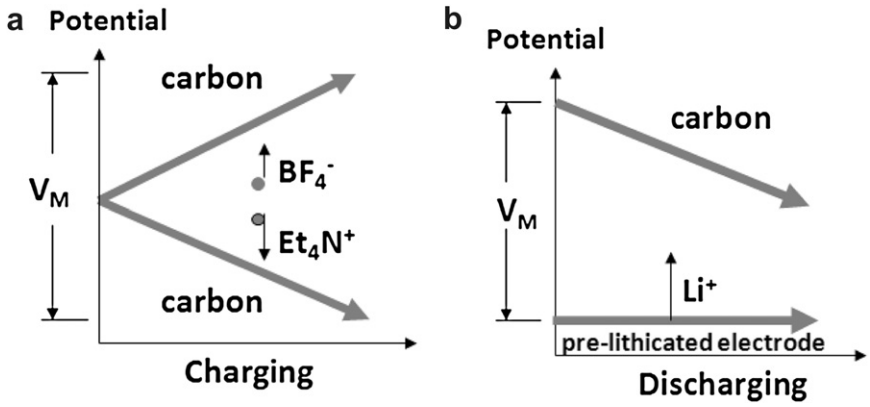

Fig. 1. Schematic potential changes of (a) symmetrical cell with two double-layer electrodes and (b) asymmetrical cell with double-layer and Li pre-inserted electrodes during the charge–discharge process. The electrolytes with salts of Et_4NBF_4 and $LiPF_6$ are assumed to be used for double-layer capacitors and asymmetrical cells, respectively.

into the electrolyte; however, for Li-ion capacitors, during the charge and discharge process, electrons move from the positive to negative electrodes and from the negative to positive electrodes, respectively, through the external load; at the same time, ions shutter between the two electrodes and the ionic concentration in the electrolyte does not change during the charge and discharge process.

2. Experimental

Fig. 2 shows the schematic diagram of the Li-ion capacitor. The anode electrode was made with mixture of hard carbon (HC), carbon black (CB), and polyvinylidene fluoride (PVDF) as binder at a ratio of 90:3:7 by weight. The cathode electrode was made with mixture of activated carbon (AC), CB, and PVDF as binder at a ratio of 85:8:7 by weight. The stabilized lithium metal powder (SLMP) was applied onto the surface of prefabricated hard carbon anode

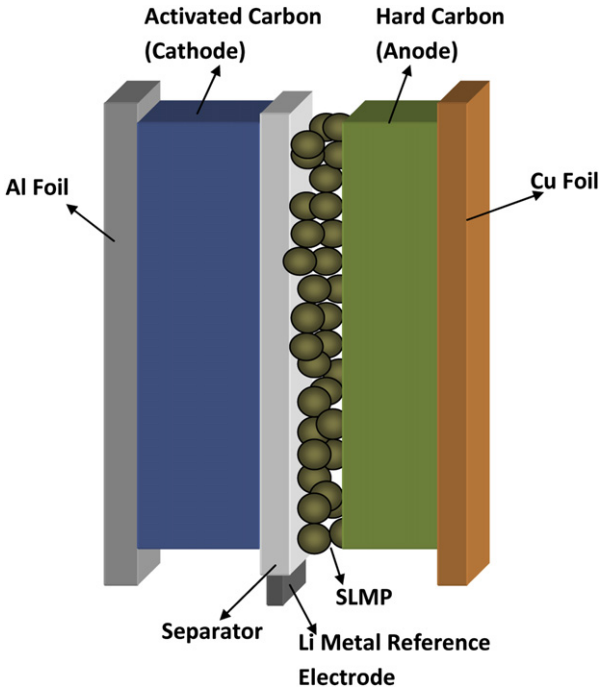

Fig. 2. A schematic diagram of an activated carbon/SLMP surface applied hard carbon Li-ion capacitor configuration.

electrodes. The SLMP, made by FMC Lithium, is a Li powder with a passivation layer at surface and can be safely handled in a dry room atmosphere. The size of the powder is in a range of 10–200 nm. The CB was added in both electrodes in order to improve the electrical conductivity. The electrolyte was 1.2 M $LiPF_6$ in ethylene carbonate (EC):diethyl carbonate (DEC):propylene carbonate (PC) at a ratio of 3:4:1 by weight. The copper and aluminium foils were used as current collectors of anode and cathode electrodes, respectively. Three-electrode Li-ion capacitor cells were assembled with Li metal as the reference electrode to show the anode and cathode potential changes versus Li^+/Li. Two-electrode Li-ion capacitor cells were assembled in order to characterize the energy density, power density, and cycle life.

A three-electrode cell was discharged and charged from 1.8 V to 3.9 V under a constant current density while the anode and cathode potentials were monitored. The two-electrode cell was discharged and charged under a constant current density for over 600 cycles and was also discharged and charged under different current densities and power densities.

3. Results and discussion

Fig. 3(a) shows the galvanostatic charge–discharge profile from a three-electrode cell in the voltage range from 1.8 to 3.9 V under a constant current density 0.2 mA cm^{-2}. The detailed material compositions of electrodes are listed in Table 1. The potential of the positive and negative electrodes has been recorded separately vs. the Li^+/Li reference electrode during the charge–discharge. It can be observed that the anode and cathode potentials swung from 0.47 to 0.12 V and 2.27 to 4.02 V vs. Li^+/Li, respectively. The potential change of the anode was much less than that of the cathode due to the large capacity of anode. Since the reversible Li-intercalation process occurred in HC anode electrode, it is obvious that the performance including the cycle life and power density would be limited by the anode electrode. Fig. 3(b) shows the voltage profile of the two-electrode cell being charged and discharged from 2.0 to 3.9 V at current density 0.8 mA cm^{-2}. The open-circuit voltage (OCV) of both the three-electrode and two-electrode cells was about 2.9 V and the specific energy is about 82 Wh kg^{-1} based on the weight of electrode materials. The weights of electrodes, separator paper, current collectors, and electrolyte in electrodes and separator were measured and listed in Table 1. Half of the weights of the current collectors were considered because in the packaged cell, both sides of current collectors were loaded with electrode materials. The specific energy of the Li-ion capacitors was estimated to be about 25 Wh kg^{-1}. It should be pointed out that the

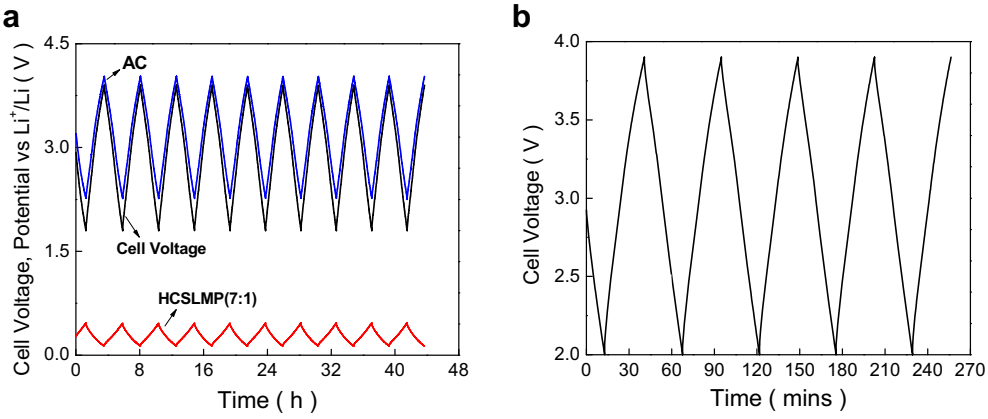

Fig. 3. Galvanostatic charge–discharge profiles of Li-ion capacitors during cycling from (a) three-electrodes test cell with Li metal reference electrode at a constant current density of 0.2 mA cm^{-2} from 1.8 to 3.9 V and (b) two-electrodes test cell at a constant current density of 0.8 mA cm^{-2} from 2.0 to 3.9 V.

Table 1
Summary of electrode and cell parameters for three-electrodes and two-electrodes cells.

Three-electrode cell	Composition	Weight (mg)	Swing voltage (V)
Anode	HC:CB:PVDF = 90:3:7	35	0.47–0.12
	SLMP on anode surface	5	
Cathode	AC:CB:PVDF = 85:8:7	17	2.27–4.02
Cell		57	1.8–3.9

Two-electrode cell	Composition	Weight (mg)
Anode	HC:CB:PVDF = 90:3:7	7
	SLMP on anode surface	1
Cathode	AC:CB:PVDF = 85:8:7	8
Separator	Celgard 3501	3.5
Electrolyte	1.2 M $LiPF_6$ EC:DEC:PC = 3:4:1	24
Current collector	Cu foil (anode)	5.5
	Al foil (cathode)	3
Total		52

AC: activated carbon, CB: carbon black, HC: hard carbon, SLMP: stabilized lithium metal powder, PVDF: polyvinylidene fluoride. The energy density is experimental values, respectively.

specific energy would be further reduced due to the requirement of package materials. The typical package efficiency is about 80% [13].

The charge transfer mechanism of Li-ion capacitors is fundamentally different to previous capacitors including traditional symmetric double-layer capacitors and asymmetric cells demonstrated by Amatucci et al. [9,10], in that less or even no salt in the electrolyte will be consumed during the capacitor cycling as shown in Fig. 1. The maximum possible energy density (or specific energy) of such kind of capacitors has been described in previous papers [11,12].

In order to obtain information concerning the long term stability of the Li-ion capacitor, the charge and discharge cycles were performed from 2.0 to 3.9 V. Fig. 4(a) shows the charge and discharge specific energy as a function of the cycle number for charge–discharge cycling and round-trip energy efficiency. It can be seen that after 600 cycles, the capacity degradation is less than 3%. Fig. 4(b) displays charge and discharge curves for the 1st, 10th, 50th, 100th, 300th and 600th cycles for the Li-ion capacitor cell. The shape of the charge and discharge curve and the charge and discharge time do not appreciably change as the cycle number increases which also demonstrate the long cycle stability for Li-ion capacitor cell. The round-trip energy efficiency closed to 100%.

The electrochemical impedance spectra (EIS) were performed to the Li-ion capacitor. These spectra were recorded in the range from 10 mHz to 1 MHz with a signal amplitude of 10 mV. Fig. 5(a) shows the EIS measured from the Li-ion capacitor at ambient temperatures of −20, 0, 20, 30, 50, and 70 °C. All EIS at different ambient temperatures were measured at cell bias voltage of 3.9 V. The EIS were also fitted by an electric equivalent circuit model [14] as shown in Fig. 5(b). The spectra contain a resistance R_s at the interception of the real axis which can be ascribed to the electrolyte, separator and contacts, and correlates with the ohmic polarization of the cell. At least three overlapping depressed semi-cycles

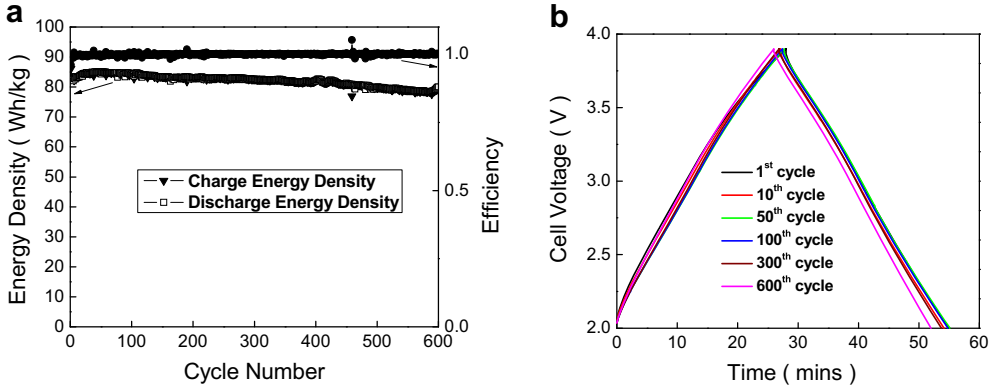

Fig. 4. (a) The specific charge and discharge energy, and the energy efficiency as a function of cycle number for the two-electrodes test cell and (b) the voltage profiles of the two-electrodes Li-ion capacitor cell for the 1st, 10th, 50th, 100th, 300th and 600th cycles.

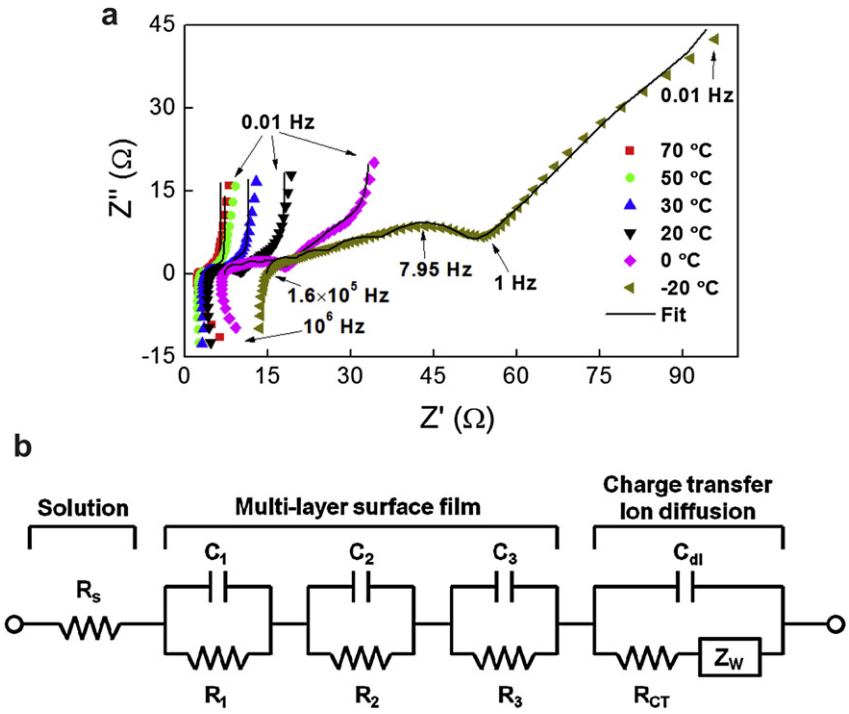

Fig. 5. (a) The EIS of Li-ion capacitor measured at different ambient temperatures, and (b) the electric equivalent circuit used to fit the EIS.

are observed at high to medium frequencies. These semi-cycles are associated with the migration of lithium ion through SEI layers which cover the electrode and have equivalent SEI resistance R_j ($j = 1–3$) and corresponding SEI capacitance C_j ($j = 1–3$). The semi-circle at mid-frequencies is associated with intercalation type reactions and is characterized by charge transfer resistance R_{CT} and the associated double-layer capacitance C_{dl}. The low frequency Warburg slope line represents the semi-infinite diffusion of Li-ion in the electrodes and was represented by Z_W. The Warburg element Z_W given by following equation [14,15]:

$$Z_W = R_W \frac{\coth(j\omega\tau_W)^p}{(j\omega\tau_W)^p}$$

Table 2 listed the fitting parameters for the cell at different ambient temperatures. It can be seen that all resistance values due to the ohmic resistance (R_s), SEI layers (R_j, $j = 1–3$), charge transfer (R_{CT}), and Warburg element (R_W) increased with decreasing temperature. This result is reasonable due to the Li-ion conductivity and diffusivity in both liquid and solid phases decreases with decreasing temperature.

Cycling performance at various charge and discharge rates for the Li-ion capacitor cell is shown in Fig. 6(a). In the first 11 cycles, the test cell was charged and discharged under 2.4C rate achieving a specific discharge energy about 82 Wh kg^{-1} with good cycle stability. When the cell was operated at the 6C and 17C charging and discharging rates, the specific discharge energies were 74 Wh kg^{-1} and 62 Wh kg^{-1} with stable cycle life, respectively. Even at the 44C rate, the cell still delivered specific discharge energy of about 48 Wh kg^{-1}, respectively. After 34 cycles, the cell still had a specific discharge energy of 82 Wh kg^{-1} when reset to 2.4C charging and discharging rate, which is almost the same as the specific discharge energy prior the high rate charge and discharge. The high rate performance and good specific energy retention at various charging and discharging rates indicate that this Li-ion capacitor cell was capable of delivering and storing high power. Fig. 6(b) shows the charge and discharge curves at current densities of 0.79 mA cm^{-2}, 1.58 mA cm^{-2}, 3.16 mA cm^{-2}, and 6.32 mA cm^{-2}. The Li-ion capacitor cell was also discharged under constant power mode and Fig. 7 shows the Ragone plot based on the weight of electrode materials only.

An EC capacitor structure with activated carbon cathode and graphite carbon anode was demonstrated previously [16]. In the previous work, no SLMP was used in the capacitor. The difference between our Li-ion capacitor and previous EC capacitors is

Table 2
Fitting parameters obtained from the cell at different ambient temperatures.

Temp	R_s (Ω)	SEI layers						Charge transfer		Warburg (Z_W)		
		R_1 (Ω)	C_1 (F)	R_2 (Ω)	C_2 (F)	R_3 (Ω)	C_3 (F)	R_{CT} (Ω)	C_{dl} (F)	R_W (Ω)	τ_W (s)	p
−20 °C	14.9	5	1.65×10^{-6}	6	2.1×10^{-5}	8.8	1.8×10^{-4}	13.8	1.4×10^{-3}	164.5	94.4	0.5
0 °C	7.2	2.8	6×10^{-6}	3.4	7.1×10^{-5}	3.8	7.2×10^{-4}	1.6	0.42	45	41.5	0.5
20 °C	4.7	2.0	9.5×10^{-6}	2.0	1.1×10^{-4}	1.1	1.4×10^{-3}	0.81	0.26	22.5	20.3	0.5
30 °C	3.7	1.3	1.9×10^{-5}	0.27	2.9×10^{-4}	0.9	3.2×10^{-4}	0.33	0.12	15.3	14.4	0.5
50 °C	2.9	0.83	3.8×10^{-5}	0.2	1.5×10^{-3}	0.1	3.6×10^{-2}	0.06	0.28	11	10.9	0.5
70 °C	2.5	0.58	7.2×10^{-5}	0.13	6.0×10^{-4}	0.096	8.6×10^{-3}	0.04	0.12	9.5	9.3	0.5

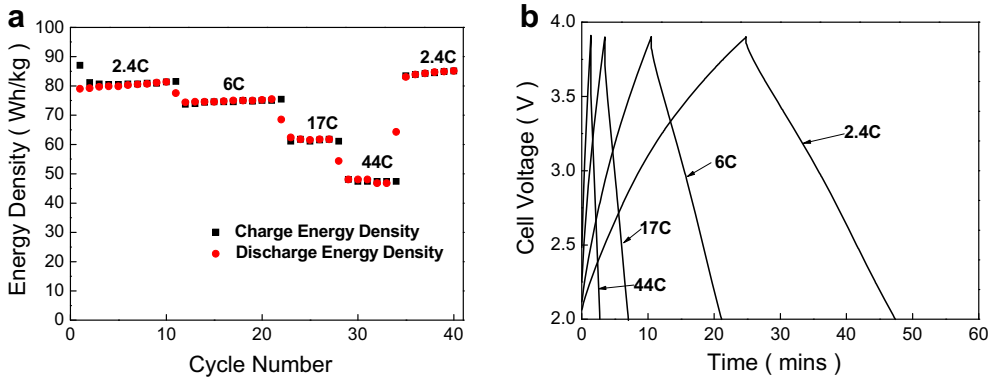

Fig. 6. (a) Cycling performance and (b) charge and discharge curves at various charge and discharge rates.

the resource of the Li ions for the electrodes. In the previous EC capacitor, the Li ions came exclusively from the electrolyte; while the Li-ion capacitor came mainly from the SLMP. In addition, the open-circuit voltage of the cell was nearly zero and the anode electrode potential was about 3 V vs. Li/Li$^+$. Fig. 8(a) shows potentials of anode and cathode electrodes vs. Li/Li$^+$ from an EC capacitor made with anode (AC 23 mg), cathode (HC 18 mg), and electrolyte (1.2 M $LiPF_6$ in EC/DEC/PC = 3/4/1 by weight). The configuration of the capacitor is similar to the Li-ion capacitors discussed above, but without SLMP in the anode electrode. It can be seen that the initial potentials of both anode and cathode electrodes were about 3 V vs. Li/Li$^+$. Due to the high potential of the anode electrode, the cathode electrode was pushed to a potential about 4.6 V vs. Li/Li$^+$ which is out of the upper limit of the electrochemical stable potential. The rapid capacitance degradation and low round-trip energy efficiency indicated non-reversible reactions occurred during the charge and discharge. The large voltage drop or jump during the current switch from charge to discharge or discharge to charge, respectively, was due to high ohmic resistance (R_s in Fig. 5(b)) contributed by the electrolyte, because the Li-ion concentration in the electrolyte was significantly reduced. The large amount of Li ions in electrolyte intercalated into HC anode during the first charge, but less than 1/3 of Li ions de-intercalated from anode.

Another carbon/carbon Li-ion capacitor configuration was also introduced with activated carbon as the cathode, graphite carbon as the anode, and Li foil as the Li-ion source for the anode [17,18]. The main difference between this work and previous one is that the Li-ion capacitor presented in this paper formulated with two electrodes-anode and cathode, just like conventional batteries and EC capacitors, but other Li-ion capacitors formulated with three electrodes-anode, cathode, and Li electrode, and pre-doped of Li to

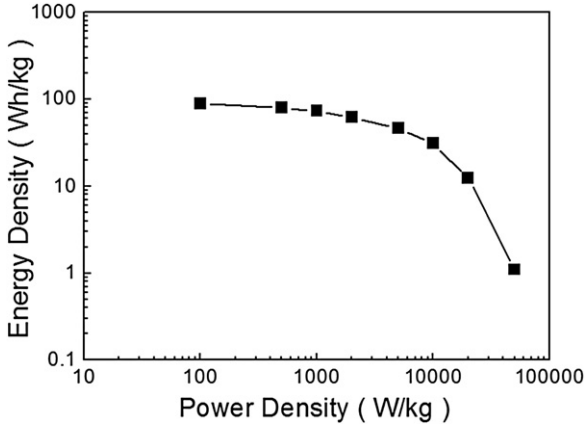

Fig. 7. The specific energy as a function of specific power based on weight of anode and cathode electrodes.

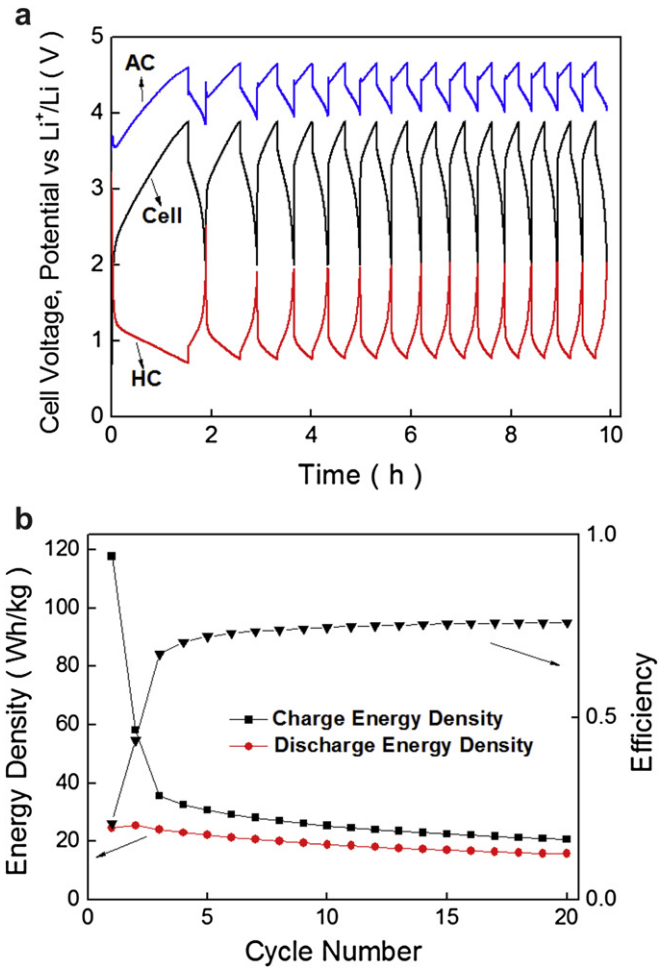

Fig. 8. Galvanostatic charge–discharge profiles of HC–AC capacitor during cycling from three-electrodes test cell with Li metal reference electrode at a constant current 0.4 mA cm^{-2} from 2.0 to 3.9 V, and (b) calculated energy density (based on electrode materials only) and round-trip energy efficiency.

anode was required. After the pre-doping, the operational principal of both Li-ion capacitors is similar.

4. Conclusion

Li-ion capacitors which consist of a Li-intercalation hard carbon with SLMP applied on surface anode electrode and double-layer capacitor type activated carbon cathode electrode were evaluated. The Li-ion capacitor is fundamentally different compared to the conventional symmetrical double-layer capacitors and asymmetrical cells, in which Li-ion capacitors do not consume electrolyte during charge and discharge cycling and can achieve much higher specific energy than conventional capacitors. The Li-ion capacitor discussed can achieve a specific energy of 82 Wh kg^{-1} based on the weight of electrodes and a specific energy of 25 Wh kg^{-1} based on the weight of combined electrodes, separator, electrolyte, and current collectors. The Li-ion capacitor has been shown to exhibit good cycle life and high specific power.

Acknowledgements

We thank Mr. Tien Duong at DOE for numerous discussion and helpful assistance.

References

[1] H. Shi, Electrochim. Acta 41 (1996) 1633.
[2] H. Nakamura, M. Okamura, in: Proceedings of the 13th International Seminar on Double Layer Capacitors, Florida Educational Seminars Inc. (2003).
[3] V.L. Pushparaj, M.M. Shaijumon, A. Kumar, S. Murugesan, L. Ci, R. Vajtai, R.J. Linhardt, O. Nalamasu, P.M. Ajayan, Proc. Natl. Acad. Sci. USA. 4 (2007) 13574.
[4] J. Chmiola, G. Yushin, Y. Gogotsi, C. Portet, P. Simon, P.L. Taberna, Science 313 (2006) 1760.
[5] J.P. Zheng, J. Huang, T.R. Jow, J. Electrochem. Soc. 144 (1997) 2026.
[6] J.P. Zheng, T.R. Jow, J. Electrochem. Soc. 144 (1997) 2417.
[7] J.P. Zheng, J. Electrochem. Soc. 150 (2003) A484.
[8] J.P. Zheng, J. Electrochem. Soc. 152 (2005) A1864.
[9] G.G. Amatucci, F. Badway, A. DuPasquier, T. Zheng, J. Electrochem. Soc. 148 (2001) A930.
[10] G.G. Amatucci, F. Badway, J. Shelburne, A. Gozdz, I. Plitz, A. DuPasquier, S.G. Menocal, in: Proceedings of the 11th International Seminar on Double Layer Capacitors, Florida Educational Seminars Inc. (2001).
[11] J.P. Zheng, J. Electrochem. Soc. 156 (2009) A500.
[12] J.P. Zheng, W.J. Cao, in: The 20th International Seminar on Double Layer Capacitors and Similar Energy Storage Devices, Florida Educational Seminars Inc. (2010).
[13] M.J. Riezenman, IEEE Spectrum 32 (May 1995) 51.
[14] P.L. Moss, G. Au, E.J. Plichta, J.P. Zheng, J. Power Sources 189 (2009) 66.
[15] M.D. Levi, G. Salitra, B. Markovsky, H. Teller, D. Aurbach, U. Heider, L. Heider, J. Electrochem. Soc. 146 (1999) 1279.
[16] V. Khomenko, E. Raymundo-Pinero, F. Beguin, J. Power Sources 177 (2008) 643.
[17] S.R. Sivakkumar, A.G. Pandolfo, Electrochim. Acta, in press.
[18] T. Aida, K. Yamada, M. Morita, Electrochem. Solid State Lett. 9 (2006) A534.